Micro-Brillouin scattering study of ferroelectric relaxor $Pb[(Zn_{1/3}Nb_{2/3})_{0.91}Ti_{0.09}]O_3$ single crystals under the electric field along the [001] direction

Do Han Kim[a)]
Graduale School of Pure and Applied Sciences, University of Tsukuba, Tsukuba, Ibaraki 305-8573, Japan

Jae-Hyeon Ko
Department of Physics, Hallym University, 39 Hallymdaehakgil, Chuncheon, Gangwondo 200-702, Korea

C. D. Feng
Shanghai Institute of Ceramics, Chinese Academy of Sciences, Shanghai, 200050, China

Seiji Kojima[b)]
Institute of Materials Science, University of Tsukuba, Tsukuba, Ibaraki 305-8573, Japan

(Received 30 March 2005; accepted 30 June 2005; published online 24 August 2005)

Electric-field effects on structural phase transitions have been studied in ferroelectric relaxor $Pb[(Zn_{1/3}Nb_{2/3})_{1-x}Ti_x]O_3$ single crystals with $x=0.09$ by the high-resolution micro-Brillouin scattering. Sharp phase transitions from cubic-to-tetragonal and then from tetragonal-to-rhombohedral phases have been observed under zero-field-cooling (ZFC) condition. For two phase-transition temperatures a noticeable thermal hysteresis was clearly observed, consistent with dielectric measurements. The temperature range of a tetragonal phase has been markedly extended under the electric field of $E=6.7$ kV/cm along the [001] direction. A large difference of the LA-mode frequency and damping between the ZFC and field-cooling processes indicated that the multidomain structure induces the increase of the acoustic damping due to the elastic scattering. In addition, it was found that the elastic stiffness coefficient c_{33} in the tetragonal coordinates shows a slight decrease. The first-order character of the cubic-to-tetragonal phase transition has been gradually changed into a second-order one under the increase of the electric field along the [001] direction, reflecting a general trend of the first-order ferroelectric phase transition. Although a clear specification of the low-temperature symmetry could not be accomplished from Brillouin scattering itself, these results give new insights into an electric-field-temperature phase diagram containing phase boundaries among cubic, tetragonal, and low-temperature phases. © *2005 American Institute of Physics*. [DOI: 10.1063/1.2008353]

I. INTRODUCTION

Lead-based relaxor ferroelectric $Pb[(Zn_{1/3}Nb_{2/3})_{1-x}Ti_x]O_3$(PZN-$x$%PT) and $Pb[(Mg_{1/3}Nb_{2/3})_{1-x}Ti_x]O_3$(PMN-$x$%PT) single crystals are promising candidates for electromechanical applications owing to their superior piezoelectric properties. High strain levels up to 1.7% in addition to electromechanical coupling constants of more than 90% were reported for [001]-oriented PZN-x%PT single crystals with the composition near the morphotrophic phase boundary (MPB) which separates a Zr-rich rhombohedral phase from a Ti-rich tetragonal one.[1] Recent investigations revealed two types of monoclinic deformation in a PZN-8%PT single crystal during the field-induced transformation with the electric field along the [001] direction in a rhombohedral phase.[2,3] Phases with a lower symmetry other than tetragonal and rhombohedral ones such as orthorhombic or monoclinic ones were also reported in other PZN-8%–9%PT and in PMN-33%–35%PT single crystals.[4–9] The intermediate monoclinic and orthorhombic phases are expected to contribute to the high piezoelectric and electromechanical responses, since they may represent the structural bridge between the tetragonal and rhombohedral phases within which the polarization vector is free to rotate.[10] Detailed phase diagrams of PZN-x%PT and PMN-x%PT single crystals near MPB have been studied resently based on synchrotron x-ray measurements.[11,12]

PZN-x%PT and PMN-x%PT single crystals near MPB have been known to exhibit two successive phase transitions from cubic-to-tetragonal and from tetragonal-to-rhombohedral phases. These two phase transitions are known to be first-order phase transitions with noticeable thermal hysteresis.[13] Very recently, Ohwada *et al.* found that the zero-field-cooled (ZFC) state of PZN-8%PT at low temperatures is not a rhombohedral but a different phase, temporarily called X.[14] Succeeding studies on PZN-x%PT and PMN-x%PT reported that the rhombohedral distortion is limited to the outer layer of the crystals at low PT concentration giving evidence of decoupling between lattice distortion and ferroelectric polarization.[15,16]

The external electric field could cause the transformation of the X phase into rhombohedral or monoclinic phases. These recent studies demonstrated that the phase diagrams of

[a)]Electronic mail: dhkim@ims.tsukuba.ac.jp
[b)]Electronic mail: kojima@bk.tsukuba.ac.jp

PZN-x%PT and PMN-x%PT, in particular, near MPB are more complicated than we have expected. It is highly desirable to look into the phase sequences of these crystals under the electric field for better understanding of the origin of giant piezoelectricity. The present study contributes to giving an E-T phase diagram of PZN-9%PT single crystals based on elastic properties measured by the high-resolution micro-Brillouin scattering technique. The temperature dependence of elastic properties of PZN-9%PT under ZFC condition and electric-field-elastic-constant hysteresis loops have already been reported on single crystals obtained from flux-grown method.[17–19] Since there has been no systematic investigation into the FC effects on PZN-9%PT single crystals, we examined the elastic properties of this composition in a large temperature range. Drastic changes in elastic properties have been observed under field-cooling condition, and phase boundaries between different symmetries have been accurately determined.

II. EXPERIMENT

PZN-x%PT single crystals were grown by the Bridgman method at Shanghai Institute of Ceramics and cut for obtaining pseudocubic crystal orientations of [100]/[010]/[001]. The crystal surfaces, perpendicular to the pseudocubic [001] direction, were polished to optical grade. Transparent indium-tin-oxide (ITO) electrodes were coated to apply an electric field. A micro-Brillouin scattering system with a 3+3 pass Sandercock tandem Fabry-Perot interferometer (FPI) has been used to measure the Brillouin spectra of PZN-9%PT crystals. An optical microscope (Olympus BH-2) was combined with the FPI to achieve a focal point of 1–2 μm. An Ar+ ion laser with a wavelength of 514.5 nm and a power of ~100 mW was used to excite the crystal. A conventional photon counting system and a multichannel analyzer were used to detect and average the signals. A free spectral range of 75 GHz was chosen, and a scan range of ±60 GHz was used.

A sample was put in a cryostat cell (THMS 600) with the stability of ~0.1 °C between 20 and 250 °C. The cryostat cell was then put on the stage of the microscope combined with a x-y translator. A high-voltage power supply (HJPM-P, Matsusada Precision, Inc.) was connected to the ITO electrodes for applying the electric field to the sample. Since we have used a backscattering geometry, the phonon propagating direction was along [001], which was the same direction of the applied dc bias field. Incident polarization was [010], and no analyzer was used for the scattered light. Before all measurements, the samples were first annealed at 550 °C for 1 h. If the Brillouin spectra are measured during cooling and heating processes without any biasing electric field, these two processes are denoted as ZFC and zero-field-heating (ZFH) processes, respectively. If the temperature dependence of the Brillouin spectra is examined under a field-cooling condition at various biasing fields, it is mentioned as field-cooling (FC) processes.

Platelet samples for dielectric measurements were independently cut from the same crystal batch, whose large surfaces were perpendicular to ⟨001⟩ and polished to optical quality. Silver or aluminum was deposited on the large surfaces as electrodes. The complex dielectric constant was measured by the impedance gain-phase analyzer (SI1260) at several frequencies. The temperature of a sample was controlled by a homemade high-temperature furnace combined with a digital temperature controller (Lakeshore 331). The typical cooling or heating rate was 0.5 K/min. For all the dielectric measurements, the amplitude of the probe sine wave was always less than 10 V/cm. Before measurements, samples were annealed for at least 1 h above the phase transition temperature to remove any memory effect of previous treatments.

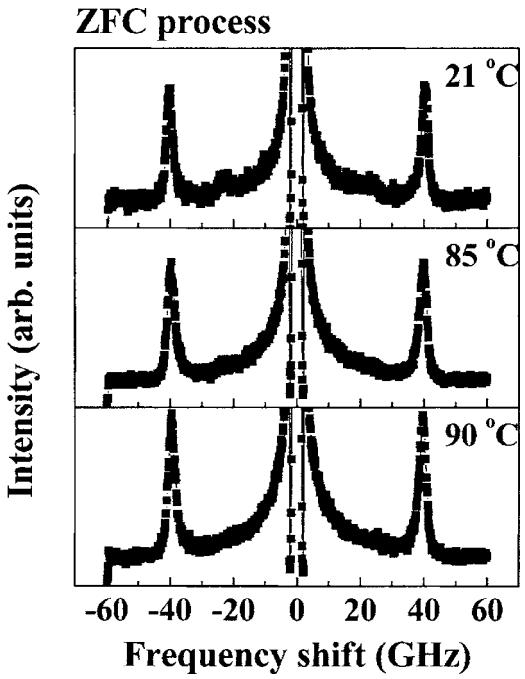

FIG. 1. Brillouin spectra of PZN-9%PT under ZFC process at selected temperatures.

III. RESULTS

Typical Brillouin spectra consisted of one longitudinal-acoustic (LA) mode, one weak transverse-acoustic (TA) mode, and a central peak (CP) as can be seen in Fig. 1, where the TA mode was noticeable only in the low-temperature rhombohedral phase below 73 °C. This result is a natural consequence from a symmetrical point of view since the TA mode is not allowed at the present scattering geometry in both cubic and tetragonal phases.[20] Figure 2 shows the temperature dependences of the mode frequency ν_{LA} and damping factor γ_{LA} of the LA mode measured during the first heating and subsequent cooling processes. The real part of the complex dielectric constant measured on cooling was also plotted for comparison. Two abrupt steplike changes in ν_{LA} and γ_{LA} are very significant at two phase-transition temperatures from cubic-to-tetragonal and tetragonal-to-rhombohedral phases, which are denoted as $T_{C\text{-}T}$ and $T_{T\text{-}R}$, respectively. Clear thermal hysteresis can be seen at both transitions, which reflects the first-order character of the two phase transitions in PZN-9%PT. The phase-transition temperatures probed by Brillouin scattering are in good agree-

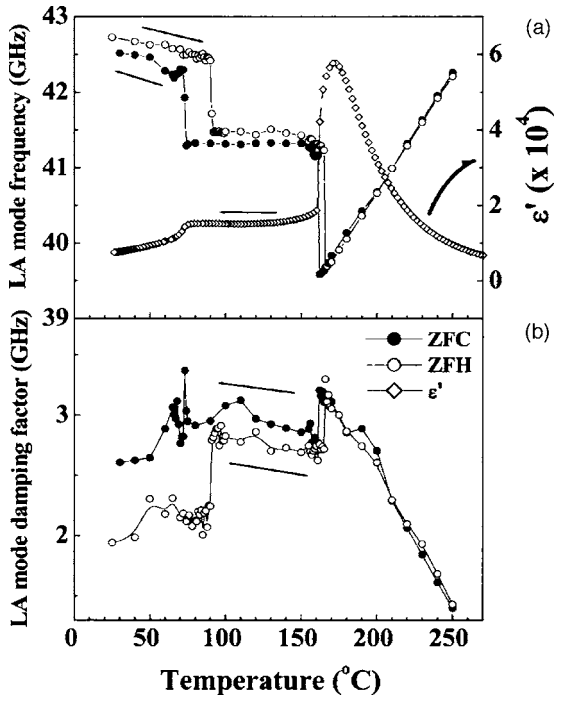

FIG. 2. (a) LA-mode frequency and (b) damping factor measured at ZFH and subsequent ZFC processes. The real part of the dielectric constant measured under ZFC is also plotted in (a) for comparison.

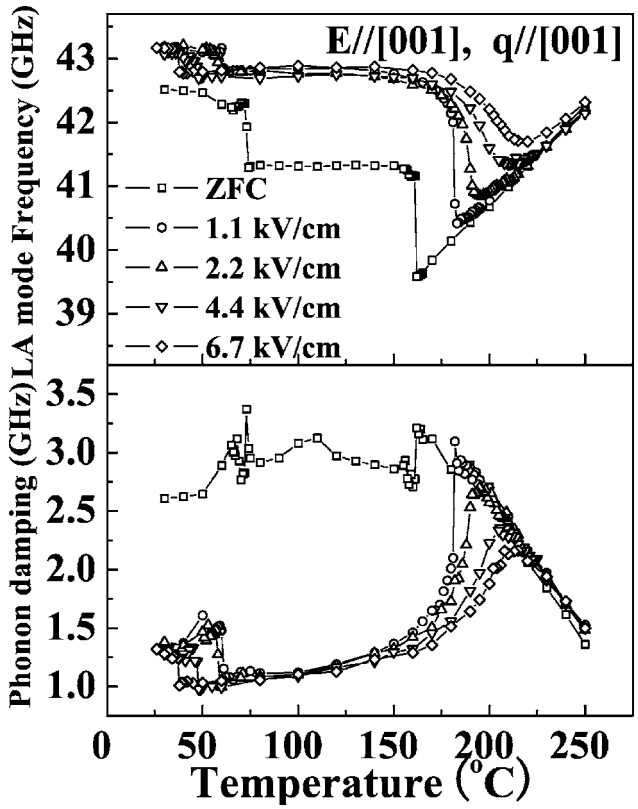

FIG. 3. (a) LA-mode frequency and (b) damping factor measured at various biasing electric fields under FC.

ment with those obtained from dielectric measurements, as shown in Fig. 2(a). Regarding the absolute values of ν_{LA} and γ_{LA} obtained on ZFH and ZFC processes, they coincide in a cubic phase, while they show noticeable differences in both tetragonal and rhombohedral phases. It has been shown that the high-resolution micro-Brillouin scattering measurements could detect the microheterogeneity of relaxor crystals and that marked positional variation in ν_{LA} and γ_{LA} could be correlated with the dynamical behaviors of the polar microregions.[17,21] The differences of ν_{LA} and γ_{LA} in both phases below $T_{C\text{-}T}$, observed at the same measured point of PZN-9%PT during heating and cooling processes, may reflect the microheterogeneity which is inherent in ferroelectric relaxors near MPB. We also found that ν_{LA} and γ_{LA} depend on the measuring position of the same crystal, similar to the case of PZN-9%PT grown by flux-grown method.[17]

Figure 3 shows ν_{LA} and γ_{LA} measured on ZFC and FC processes under various electric fields. Under the electric field up to 6.7 kV/cm along the [001] direction, the two phase transitions from cubic to tetragonal and then to another low-temperature phase can still be seen. However, significant changes in both ν_{LA} and γ_{LA} have occurred between two processes: (1) The temperature range of the tetragonal phase is significantly extended into both high- and low-temperature sides under the electric field along the [001] direction. (2) The discontinuity at $T_{C\text{-}T}$ under ZFC process is smeared out during the FC process as the amplitude of the biasing electric field increases. (3) The γ_{LA} has been greatly suppressed by the application of the poling field probably due to the marked decrease of scattering at domain walls.

It is well known for a first-order ferroelectric phase transition that a ferroelectric phase can be induced by an external electric field along a ferroelectric axis at temperatures above the Curie temperature.[22] $T_{C\text{-}T}$ has been increased under 6.7 kV/cm from 162 to 209 °C, at which the discontinuity of ferroelectric properties seems to disappear. It is understood that the applied electric field of about 6.7 kV/cm might be high enough to remove the discontinuity of the cubic-to-tetragonal transition point. In contrast, the discontinuity of the tetragonal-to-rhombohedral phase transition still remains under the electric field up to 6.7 kV/cm. Since the electric field along the [001] direction is a conjugate field to a spontaneous polarization of the uniaxial ferroelectric tetragonal phase of PZN-9%PT, this tetragonal phase becomes more stabilized and wider in the temperature window under FC condition. A similar variation of the elastic properties is also expected owing to the piezoelectric coupling of polarization and strain.

Although the applied electric field of 6.7 kV/cm may not be enough for inducing a complete monodomain in the present PZN-9%PT in the tetragonal symmetry due to the very complex relaxor behaviors, the tetragonal phase induced under the FC process would approach closer to a single-domain state. ν_{LA} measured under the ZFC process is larger than that measured with the biasing field. The electric-field dependence of ν_{LA} is very small from 1.1 to 6.7 kV/cm. It demonstrates that the elastic stiffness coefficient depends on whether the sample is free to deform in the quasimonodomain state having a smaller number of macrodomains or is elastically constrained in polydomain state. In addition, γ_{LA} of the single domain state is usually much smaller than the value in the multidomain state. This indicates that the multidomain structure of the PZN-9%PT single crystal con-

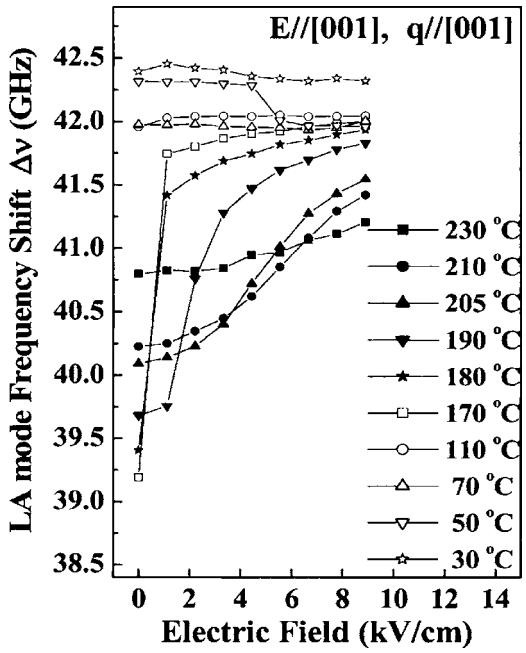

FIG. 4. Electric-field dependence of the LA-mode frequency at selected temperatures.

tributes to the hypersonic attenuation and thus the attenuation should become smaller if the crystal is transformed into a quasimonodomain state or a state with fewer domains under poling field.

In order to look into the field-induced effects in more detail, ν_{LA} has been examined as a function of the biasing electric field at constant temperatures as shown in Fig. 4. At temperatures far above $T_{C\text{-}T} \sim 162\ ^{\circ}\mathrm{C}$, ν_{LA} induced by the biasing field gradually approaches the value of the tetragonal phase. However, as the temperature approaches closer to $T_{C\text{-}T}$, the change of ν_{LA} becomes more drastic. At temperatures of 180 and 170 °C above $T_{C\text{-}T}$, the smallest applied fields of 1.1 kV/cm was enough for making ν_{LA} equal to the value of a tetragonal phase, consistent with the result as shown in Fig. 3. On the other hand, a tetragonal phase is induced from a rhombohedral phase at 50 °C by applying an electric field of 6.7 kV/cm. Only at 30 °C can a low-temperature rhombohedral phase be stable under the biasing field up to 6.7 kV/cm.

IV. DISCUSSION

Using high-resolutuion micro-Brillouin scattering, an *E-T* phase diagram of PZN-9%PT can be constructed from the present study by observing the changes of ν_{LA} as a function of the temperature under the constant biasing field, as shown in Fig. 5. Due to the limitation of the present study, the phase of lowest temperature could not be determined and only phase boundaries among cubic (C), tetragonal (T), and low-temperature phases were shown in the same figure. The change of the Curie temperature (T_c) under the applied field gives the values of $dT_c/dE \sim 7.8 \times 10^{-3}$ and -5.8×10^{-3} K cm/V for the cubic-tetragonal and tetragonal-low-temperature phase boundaries, respectively. The former value is much larger than that of a cubic-to-tetragonal phase transition in $BaTiO_3$, where $dT_c/dE \sim 1.6 \times 10^{-3}$ K cm/V.[23]

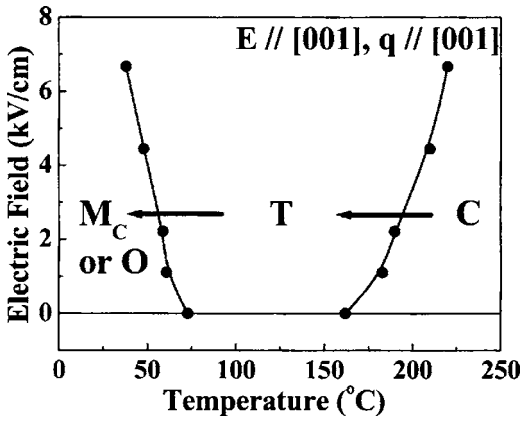

FIG. 5. Electric field vs temperature phase diagram determined from the discontinuity of LA-mode frequency measured under FC.

This phase diagram shows a large difference in the slope of the tetragonal-rhombohedral phase boundary compared to that of PZN-8%PT suggested by Ohwada *et al.*[14] It is close to the vertical in PZN-8%PT, while the change of T_c due to the electric field is much larger in PZN-9%PT. It means that the tetragonal phase of PZN-9%PT becomes more stable than PZN-8%PT on cooling under the biasing electric field along the [001] direction. The compositions of both PZN-8%PT and PZN-9%PT are located near the MPB. Compositions near MPB are characterized by superior polarizability and piezoelectricity arising from the coupling between quasidegenerate energy states, which is believed to be the origin of orthorhombic or monoclinic phases observed in PZN-x%PT of MPB compositions. A significant difference of *E-T* phase diagrams between PZN-8%PT and PZN-9%PT of the present study exhibits that the quasidegenerate energy states can be greatly modified by a slight change of the Ti composition and an external conjugate field coupled to spontaneous polarization in a tetragonal phase.

As to the low-temperature symmetry of PZN-9%PT, it cannot be determined from the present study. If we consider previous scattering experiments, it is probable that a change from a tetragonal phase into a monoclinic M_c or an orthorhombic phase might be induced by the field-cooling process in PZN-9%PT.[3,4,11,14] Further studies are necessary for improving our understanding of field-induced phases of PZN-x%PT near MPB compositions.

V. CONCLUSIONS

Variation of phase-transition behaviors has been examined in PZN-9%PT under the electric field along the [001] direction by the high-resolution micro-Brillouin scattering. Very sharp steplike changes in both LA-mode frequency and damping factor have been observed in ZFH and ZFC processes. The significant thermal hysteresis was observed in cubic-to-tetragonal and tetragonal-to-rhombohedral phase transitions. The absolute values of ν_{LA} and γ_{LA} depended on the thermal history, which may reflect the microheterogeneity of relaxor ferroelectrics. The first-order nature of the cubic-to-tetragonal phase transition seemed to disappear at the poling field of 6.7 kV/cm along the [001] direction, while the sharp steplike transition from a tetragonal to a low-

temperature phase still remained. The temperature range of a tetragonal phase of PZN-9%PT has been significantly widened under the electric field along [001] into both low-temperature and high-temperature sides, which is in contrast to the situation of PZN-8%PT.[14] A new electric-field-temperature phase diagram of PZN-9%PT has been determined based on the changes of the phase-transition temperatures.

ACKNOWLEDGMENT

This work was supported in part by the 21st Century COE (Center of Excellence) Program "Promotion of Creative Interdisciplinary Materials Science for Novel Function" under MEXT (the Ministry of Education, Culture, Sports, Science, and Technology) Japan.

[1]S.-E. Park and T. R. Shrout, J. Appl. Phys. **82**, 1804 (1997).
[2]B. Noheda, D. E. Cox, G. Shirane, S.-E. Park, L. E. Cross, and Z. Zhong, Phys. Rev. Lett. **86**, 3891 (2001).
[3]K. Ohwada, K. Hirota, P. W. Rehrig, P. M. Gehring, B. Noheda, Y. Fujii, S.-E. Park, and G. Shirane, J. Phys. Soc. Jpn. **70**, 2778 (2001).
[4]D. Viehland, J. Appl. Phys. **88**, 4794 (2000).
[5]D. E. Cox, B. Noheda, G. Shirane, Y. Uesu, K. Fujishiro, and Y. Yamada, Appl. Phys. Lett. **79**, 400 (2001).
[6]J.-M. Kiat, Y. Uesu, B. Dkhil, M. Matsuda, C. Malibert, and G. Calvarin, Phys. Rev. B **65**, 064106 (2002).
[7]G. Xu, H. Luo, H. Xu, and Z. Yin, Phys. Rev. B **64**, 020102 (2001).
[8]Z.-G. Ye, B. Noheda, M. Dong, D. Cox, and G. Shirane, Phys. Rev. B **64**, 184114 (2001).
[9]A. K. Singh and D. Pandey, J. Phys.: Condens. Matter **13**, L931 (2001).
[10]H. Fu and R. E. Cohen, Nature (London) **403**, 281 (2000).
[11]D. La-Orauttapong, B. Noheda, Z.-G. Ye, P. M. Gehring, J. Toulouse, D. E. Cox, and G. Shirane, Phys. Rev. B **65**, 144101 (2002).
[12]B. Noheda, D. E. Cox, G. Shirane, J. Gao, and Z.-G. Ye, Phys. Rev. B **66**, 054104 (2002).
[13]J. Kuwata, K. Uchino, and S. Nomura, Jpn. J. Appl. Phys., Part 1 **21**, 1298 (1982).
[14]K. Ohwada, K. Hirota, P. W. Rehrig, Y. Fujii, and G. Shirane, Phys. Rev. B **67**, 094111 (2003).
[15]G. Xu, Z. Zhong, Y. Bing, Z.-G. Ye, C. Stock, and G. Shirane, Phys. Rev. B **67**, 104102 (2003).
[16]G. Xu, H. Hiraka, G. Shirane, and K. Ohwada, Appl. Phys. Lett. **84**, 3975 (2004).
[17]F. M. Jiang and S. Kojima, Ferroelectrics **266**, 355 (2002).
[18]J.-H. Ko and S. Kojima, Appl. Phys. Lett. **81**, 1077 (2002).
[19]J.-H. Ko, D. H. Kim, and S. Kojima, Appl. Phys. Lett. **83**, 2037 (2003).
[20]R. Vacher and L. Boyer, Phys. Rev. B **6**, 639 (1972).
[21]F. M. Jiang and S. Kojima, Appl. Phys. Lett. **77**, 1271 (2000).
[22]M. E. Lines and A. M. Glass, *Priciples and Applications of Ferroelectrics and Related Materials* (Clarendon, Oxford, 1977).
[23]K. Kawabe, J. Phys. Soc. Jpn. **14**, 1755 (1959).